AIMS Mathematics, 7(1): 1257–1272.
DOI: 10.3934/math.2022074
Received: 20 May 2021
Accepted: 18 October 2021
Published: 22 October 2021

http://www.aimspress.com/journal/Math

Research article

Stress analysis of elastic bi-materials by using the localized method of fundamental solutions

Juan Wang[1], Wenzhen Qu[1,2,*], Xiao Wang[1] and Rui-Ping Xu[1]

[1] School of Mathematics and Statistics, Qingdao University, Qingdao 266071, China
[2] Institute of Mechanics for Multifunctional Materials and Structures, Qingdao University, Qingdao 266071, China

* **Correspondence:** Email: qwzxx007@163.com.

Abstract: The localized method of fundamental solutions belongs to the family of meshless collocation methods and now has been successfully tried for many kinds of engineering problems. In the method, the whole computational domain is divided into a set of overlapping local subdomains where the classical method of fundamental solutions and the moving least square method are applied. The method produces sparse and banded stiffness matrix which makes it possible to perform large-scale simulations on a desktop computer. In this paper, we document the first attempt to apply the method for the stress analysis of two-dimensional elastic bi-materials. The multi-domain technique is employed to handle the non-homogeneity of the bi-materials. Along the interface of the bi-material, the displacement continuity and traction equilibrium conditions are applied. Several representative numerical examples are presented and discussed to illustrate the accuracy and efficiency of the present approach.

Keywords: meshless method; localized method of fundamental solutions; domain decomposition technique; multi-layered elastic materials; stress analysis
Mathematics Subject Classification: 35E20, 65N22

1. Introduction

The multi-layered materials containing single or multiple layers have been widely synthesized, designed and utilized in industrial application to improve machining performance [1–4]. The well-established and widely applied finite element (FEM), finite difference (FDM) and boundary

element (BEM) methods offer without doubt many advantages in solving multi-layered problems due to their flexibilities in dealing with the geometry, loading type and nonlinearities of the coating layers [5–8]. The methods themselves, however, have also many inherent shortcomings especially when a re-meshing is required or when the elements become highly distorted [9–15].

Over the past two decades, some considerable effort was devoted to developing novel computational algorithms that circumvent the non-trivial tasks of FEM and/or BEM mesh generation [16–20]. This led to the development of various meshless methods. For an overview of the state of the art, we refer the interested readers to Refs. [21–27], as well as the references therein. Among these methods, the method of fundamental solutions (MFS) is a popular and robust boundary-type meshless method for the solution of certain boundary value problems [11,28]. The advantages of the method have been summarized by many researchers, see for example, Refs. [29–31]. In 2001, Berger and Karageorghis [32] demonstrated the use of the MFS for solving the layered elastic materials. Berger, Karageorghis and Martin [33] applied an enriched MFS approach for fracture mechanics analysis of cracked elastic structures. The use of the MFS with dual reciprocity approach for some problems in elasticity was reported by Medeiros et al. [34]. Karageorghis and Fairweather [35–37] presented a MFS-based method for axisymmetric elasticity problems. Karageorghis, Lesnic and Marin [38] applied the MFS for three-dimensional (3D) inverse geometric elasticity problems. Error analysis of the MFS for linear elastostatics has been given by Li et al. [39]. Liu and Šarler proposed a non-singular MFS for anisotropic elasticity problems [40–43]. Marin proposed a regularized MFS for boundary identification in two-dimensional isotropic linear elasticity problems [44,45]. Poullikkas et al. [46] demonstrated the use of the MFS for solving 3D elastic problems. Similar to the BEM-based methods, the MFS, however, produces dense and non-symmetric system matrices which makes the method difficulty for large-scale engineering simulations. During the past few years, the localized version of the MFS, named as the localized MFS (LMFS), has been proposed to improve the computational efficiency of the classical MFS. The method was firstly proposed by Fan et al. [47] in 2019 and was later essentially improved and extended by many other others [21,48–52]. Different to the classical MFS, in the LMFS the entire domain should be firstly divided into a set of overlapping local subdomains. In each of the subdomain, the classical MFS approximation and a moving least square (MLS) technique are applied to construct the local system of linear equations. The method will finally produce a sparse and banded matrix system which can be solved quickly by using various sparse matrix solvers.

This paper makes the first attempt to further extend the method for stress analysis in linear elastic bi-materials. Different to the previous published work [53] where the elastic biomaterials were modelled by using the generalized finite difference method (GFDM), the present method uses the fundamental solutions as the basic function, and therefore, the method keeps the merits of high accuracy and easy programming as compared to the GFDM. A non-overlapping multi-domain technique is employed to handle the non-homogeneity of the bi-materials. Along the interface of the bi-material, the displacement continuity and traction equilibrium conditions are applied. The present LMFS approach based on the multi-domain technique can be easily implemented into any existing MFS/LMFS codes. A brief outline of the rest of the paper is organized as follows. In Section 2, the LMFS and its numerical implementation are briefly introduced. The multi-domain LMFS formulation for stress analysis of bi-materials is presented in Section 3. Next in Section 4, three benchmark examples are studied to validate the performances of the present method. Finally, some conclusions and remarks are provided in Section 5.

2. Problem statement and the LMFS in linear elasticity

2.1. Problem statement

The governing equations for a homogeneous, isotropic and linear elasticity solid Ω can be written as (under plane strain conditions) [4,54,55]

$$\left\{2\frac{1-\nu}{1-2\nu}\right\}\frac{\partial^2 u_1(\boldsymbol{x})}{\partial x_1^2}+\frac{\partial^2 u_1(\boldsymbol{x})}{\partial x_2^2}+\left\{\frac{1}{1-2\nu}\right\}\frac{\partial^2 u_2(\boldsymbol{x})}{\partial x_1 \partial x_2}=f_1(\boldsymbol{x}), \tag{1}$$

$$\left\{\frac{1}{1-2\nu}\right\}\frac{\partial^2 u_1(\boldsymbol{x})}{\partial x_1 \partial x_2}+\frac{\partial^2 u_2(\boldsymbol{x})}{\partial x_1^2}+\left\{2\frac{1-\nu}{1-2\nu}\right\}\frac{\partial^2 u_2(\boldsymbol{x})}{\partial x_2^2}=f_2(\boldsymbol{x}), \tag{2}$$

subject to the boundary conditions

$$u_i(\boldsymbol{x})=\overline{u}_i(\boldsymbol{x}) \quad \boldsymbol{x}\in\Gamma_u \quad (\textit{Displacements}), \tag{3}$$

$$t_i(\boldsymbol{x})=\sigma_{ij}(\boldsymbol{x})n_j(\boldsymbol{x})=\overline{t}_i(\boldsymbol{x}) \quad \boldsymbol{x}\in\Gamma_t \quad (\textit{Tractions}), \tag{4}$$

where $u_i(\boldsymbol{x})$ and $t_i(\boldsymbol{x})$, $i=1,2$, are the displacement and traction components, $f_1(\boldsymbol{x})$ and $f_2(\boldsymbol{x})$ are body forces, ν denotes the Poisson's ratio of the material, $n_j(\boldsymbol{x})$, $j=1,2$, stand for the outward unit normal vector, $\overline{u}_i$ and $\overline{t}_i$ represent the prescribed boundary conditions. Here and in the following, the classical Einstein's notation for summation over repeated subscripts is employed. The strains $\varepsilon_{ij}(\boldsymbol{x})$ and stresses $\sigma_{ij}(\boldsymbol{x})$ are related to the displacements by:

$$\varepsilon_{ij}(\boldsymbol{x})=\frac{1}{2}\left\{\frac{\partial u_i(\boldsymbol{x})}{\partial x_j}+\frac{\partial u_j(\boldsymbol{x})}{\partial x_i}\right\}, \tag{5}$$

$$\sigma_{ij}(\boldsymbol{x})=2G\left(\varepsilon_{ij}(\boldsymbol{x})+\frac{\nu}{1-2\nu}\varepsilon_{kk}(\boldsymbol{x})\delta_{ij}\right), \tag{6}$$

where G is the shear modulus of the material and δ_{ij} denotes the well-known Kronecker delta. The boundary tractions (4) are related to stresses by:

$$t_i(\boldsymbol{x})=\sigma_{ij}(\boldsymbol{x})n_j(\boldsymbol{x}), \quad \boldsymbol{x}\in\Gamma. \tag{7}$$

2.2. The LMFS formulation for linear elasticity problems

In the LMFS, a cloud of points is firstly scatted inside the entire computational domain (see Figure 1). And the method defines a set of overlapping local subdomains and matches the solutions in each of the subdomain by using the classical MFS approximation. For each node $\boldsymbol{x}^{(0)}=\left(x_1^{(0)}, x_2^{(0)}\right)$ inside the

computational domain, named as the *central node*, the N_s nearest points $\boldsymbol{x}^{(i)}=\left(x_1^{(i)}, x_2^{(i)}\right)$ around $\boldsymbol{x}^{(0)}$ should be found. Then the concept of the local subdomain Ω_s refers to the small area that contains $\boldsymbol{x}^{(0)}$ and $\left\{\boldsymbol{x}^{(i)}\right\}_{i=1}^{N_s}$. Applying the classical MFS formulation to each point inside the local subdomain, the following approximations for displacements can be obtained:

$$u_1\left(\boldsymbol{x}\right)=\sum_{n=1}^{M}\left[\alpha_1^{(n)}U_{11}\left(\boldsymbol{x},\boldsymbol{s}^{(n)}\right)+\alpha_2^{(n)}U_{12}\left(\boldsymbol{x},\boldsymbol{s}^{(n)}\right)\right], \tag{8}$$

$$u_2\left(\boldsymbol{x}\right)=\sum_{n=1}^{M}\left[\alpha_1^{(n)}U_{21}\left(\boldsymbol{x},\boldsymbol{s}^{(n)}\right)+\alpha_2^{(n)}U_{22}\left(\boldsymbol{x},\boldsymbol{s}^{(n)}\right)\right], \tag{9}$$

where $\boldsymbol{x}\in\Omega_s$, $\boldsymbol{s}^{(n)}$ stands for the source points uniformly distributed on a local artificial circle with radius R_s and centered at $\boldsymbol{x}^{(0)}$ (see Figure 1), M is the number of source points, $\{\alpha_j^{(n)}\}_{n=1}^{M}$ are unknown coefficients, and

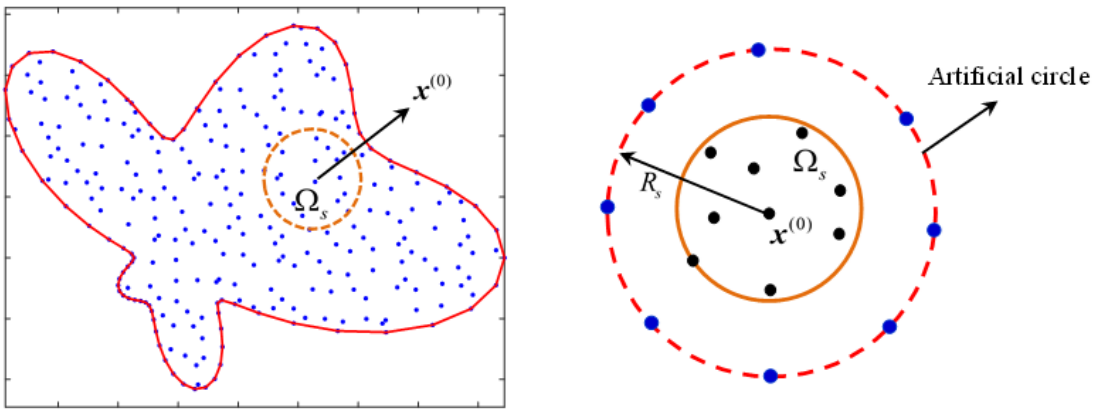

Figure 1. Geometry of the computational domain and the schematic diagram of the local subdomain.

$$U_{ij}\left(\boldsymbol{x},\boldsymbol{s}\right)=\frac{1}{8\pi G\left(1-\nu\right)}\left[\left(3-4\nu\right)\ln\left(\frac{1}{r}\right)\delta_{ij}+r_{,i}r_{,j}\right], \tag{10}$$

are fundamental solutions for displacements [5,55,56]. It is noted that the radius R_s of the artificial circle is a parameter which should be manually determined by the user. Substituting the coordinates of N_s+1 points inside Ω_s to Eqs (8) and (9) will result in the following system of equations:

$$\begin{bmatrix}\boldsymbol{u}_1\\ \boldsymbol{u}_2\end{bmatrix}_{2(N_s+1)\times 1}=\begin{bmatrix}\boldsymbol{U}_{11} & \boldsymbol{U}_{12}\\ \boldsymbol{U}_{21} & \boldsymbol{U}_{22}\end{bmatrix}_{2(N_s+1)\times 2M}\begin{bmatrix}\boldsymbol{\alpha}_1\\ \boldsymbol{\alpha}_2\end{bmatrix}_{2M\times 1}, \tag{11}$$

where $[\boldsymbol{u}_1\ \ \boldsymbol{u}_2]^T=\left[u_1\left(\boldsymbol{x}^{(0)}\right),u_1\left(\boldsymbol{x}^{(1)}\right),...,u_1\left(\boldsymbol{x}^{(N_s)}\right),u_2\left(\boldsymbol{x}^{(0)}\right),u_2\left(\boldsymbol{x}^{(1)}\right),...,u_2\left(\boldsymbol{x}^{(N_s)}\right)\right]^T$ is the vector of displacements, $[\boldsymbol{\alpha}_1\ \ \boldsymbol{\alpha}_2]^T=[\alpha_1^{(1)},...,\alpha_1^{(M)},\alpha_2^{(1)},...,\alpha_2^{(M)}]^T$ stands for the vector of unknown coefficients. According to equation (11), the unknown coefficients $[\boldsymbol{\alpha}_1\ \ \boldsymbol{\alpha}_2]^T$ can be expressed as:

$$\begin{bmatrix}\boldsymbol{\alpha}_1\\ \boldsymbol{\alpha}_2\end{bmatrix}=\begin{bmatrix}\boldsymbol{U}_{11} & \boldsymbol{U}_{12}\\ \boldsymbol{U}_{21} & \boldsymbol{U}_{22}\end{bmatrix}^{-1}\begin{bmatrix}\boldsymbol{u}_1\\ \boldsymbol{u}_2\end{bmatrix}, \tag{12}$$

or for briefly:

$$\boldsymbol{\alpha}=\boldsymbol{U}^{-1}\boldsymbol{u}, \tag{13}$$

where $\boldsymbol{\alpha}=[\boldsymbol{\alpha}_1\ \ \boldsymbol{\alpha}_2]^T$, $\boldsymbol{u}=[\boldsymbol{u}_1\ \ \boldsymbol{u}_2]^T$ and $\boldsymbol{U}=\left\{\boldsymbol{U}_{ij}\right\}_{i,j=1,2}$. The explicit expressions of unknown coefficients $\boldsymbol{\alpha}=[\boldsymbol{\alpha}_1\ \ \boldsymbol{\alpha}_2]^T$ can now be calculated by a linear combination of function values at the N_s+1 points located inside Ω_s. In our computations, we choose $N_s=2M$ and the final system of Eq (13) is overdetermined, which can be solved in a least-squares sense using various matrix solvers. The displacements at the central node $\boldsymbol{x}^{(0)}$ can now be calculated by substituting $\boldsymbol{\alpha}=\boldsymbol{U}^{-1}\boldsymbol{u}$ again into Eqs (8) and (9) as follows:

$$\begin{aligned}u_1^{(0)}&=u_1\left(\boldsymbol{x}^{(0)}\right)=\left[\boldsymbol{h}_{11}\ \ \boldsymbol{h}_{12}\right]\begin{bmatrix}\boldsymbol{\alpha}_1\\ \boldsymbol{\alpha}_2\end{bmatrix}=\left[\boldsymbol{h}_{11}\ \ \boldsymbol{h}_{12}\right]\begin{bmatrix}\boldsymbol{U}_{11} & \boldsymbol{U}_{12}\\ \boldsymbol{U}_{21} & \boldsymbol{U}_{22}\end{bmatrix}^{-1}\begin{bmatrix}\boldsymbol{u}_1\\ \boldsymbol{u}_2\end{bmatrix}\\ &=\sum_{n=0}^{N_s}\left[\omega_{11}^{(n)}u_1^{(n)}+\omega_{12}^{(n)}u_2^{(n)}\right],\end{aligned} \tag{14}$$

$$\begin{aligned}u_2^{(0)}&=u_2\left(\boldsymbol{x}^{(0)}\right)=\left[\boldsymbol{h}_{21}\ \ \boldsymbol{h}_{22}\right]\begin{bmatrix}\boldsymbol{\alpha}_1\\ \boldsymbol{\alpha}_2\end{bmatrix}=\left[\boldsymbol{h}_{21}\ \ \boldsymbol{h}_{22}\right]\begin{bmatrix}\boldsymbol{U}_{11} & \boldsymbol{U}_{12}\\ \boldsymbol{U}_{21} & \boldsymbol{U}_{22}\end{bmatrix}^{-1}\begin{bmatrix}\boldsymbol{u}_1\\ \boldsymbol{u}_2\end{bmatrix}\\ &=\sum_{n=0}^{N_s}\left[\omega_{21}^{(n)}u_1^{(n)}+\omega_{22}^{(n)}u_2^{(n)}\right],\end{aligned} \tag{15}$$

where $[\boldsymbol{h}_{i1}\ \ \boldsymbol{h}_{i2}]=\left[U_{i1}\left(\boldsymbol{x}^{(0)},\boldsymbol{s}^{(1)}\right),...,U_{i1}\left(\boldsymbol{x}^{(0)},\boldsymbol{s}^{(M)}\right),U_{i2}\left(\boldsymbol{x}^{(0)},\boldsymbol{s}^{(1)}\right),...,U_{i2}\left(\boldsymbol{x}^{(0)},\boldsymbol{s}^{(M)}\right)\right]$ denotes the vector of fundamental solutions at point $\boldsymbol{x}^{(0)}$, and $\left\{\omega_{ij}^{(n)}\right\}_{i,j=1,2}$ are the weighing coefficients. Note that every node inside the computational domain should be regarded to be a central node and the above numerical procedures should be repeated for every node. Now let's form the final linear system of equations. Firstly, suppose n_i, n_{b1} and n_{b2} are the numbers of points distributed inside the domain and on the boundary with displacement and traction conditions, respectively. To enforce the satisfaction of Eqs (14) and (15) at every interior node yield the following linear system:

$$u_1^{(i)}-\sum_{n=0}^{N_s}\left[\omega_{11}^{(n)}u_1^{(n)}+\omega_{12}^{(n)}u_2^{(n)}\right]=0,\quad i=1,2,...,n_i, \tag{16}$$

$$u_2^{(i)} - \sum_{n=0}^{N_s} \left[\omega_{21}^{(n)} u_1^{(n)} + \omega_{22}^{(n)} u_2^{(n)} \right] = 0, \quad i = 1, 2, ..., n_i. \tag{17}$$

The boundary points should satisfy the given boundary conditions. For node with displacement conditions, the following linear system of equations can be obtained:

$$u_1^{(i)} = \bar{u}_1^{(i)}, \quad i = n_i + 1, ..., n_i + n_{b1}, \tag{18}$$

$$u_2^{(i)} = \bar{u}_2^{(i)}, \quad i = n_i + 1, ..., n_i + n_{b1}. \tag{19}$$

Similarly, for points with traction boundary conditions, another system of linear algebraic equations can be obtained [55]. By combining the above systems of equations, the following spare and banded linear algebraic equations can be formed:

$$\boldsymbol{A}\boldsymbol{u} = \boldsymbol{B}, \tag{20}$$

where $\boldsymbol{A}_{2N\times 2N}$ is the coefficient matrix, $\boldsymbol{u} = [\boldsymbol{u}_1\ \boldsymbol{u}_2]^T = [u_1^{(1)}, ..., u_1^{(N)}, u_2^{(1)}, ..., u_2^{(N)}]^T$ is the vector of unknown displacements at every node, and $\boldsymbol{B}_{2N\times 1}$ is the vector of the corresponding boundary conditions. Both the direct matrix inverse method and the moving least square approximation can be used to solve the final system of equations. Here, the direct matrix inverse method is used. On solving this system of equations, the numerical solutions of displacements at every node inside the entire domain can be obtained. Once all displacements are solved, the stresses can be obtained by replacing the displacement fundamental solutions with these for stresses, we refer the interested readers for Refs. [55,57] for further details.

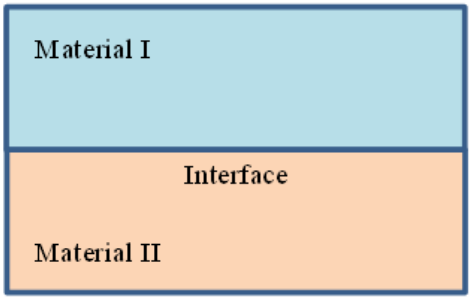

Figure 2. Multi-domain technique for a bi-material domain.

3. The multi-domain LMFS for bi-materials

The aforementioned numerical procedures are derived for homogeneous materials, a multi-domain technique [53,54] is used here to solve the bi-material problems. As shown in Figure 2, the bi-material considered here is divided into two subdomains along the interface, which are respectively homogeneous and isotropic, with the upper layer as the subdomain Ω_1 and the lower as the

subdomain Ω_2. The final system of equations can be formed by assembling equations written for each subdomain, based on the displacement continuity and traction equilibrium conditions along the interface of the bi-material. Application of the LMFS formulation to both subdomains will result in the following matrix equations:

$$\begin{bmatrix} \boldsymbol{A}^1 \\ \boldsymbol{G}_{\mathrm{I}}^1 \\ \boldsymbol{H}_{\mathrm{I}}^1 \end{bmatrix} \begin{pmatrix} \{\boldsymbol{u}^1\} \\ \{\boldsymbol{u}_{\mathrm{I}}^1\} \end{pmatrix} = \begin{bmatrix} \boldsymbol{B}^1 \\ \boldsymbol{U}_{\mathrm{I}}^1 \\ \boldsymbol{T}_{\mathrm{I}}^1 \end{bmatrix}, \tag{21}$$

for the subdomain Ω_1 and

$$\begin{bmatrix} \boldsymbol{A}^2 \\ \boldsymbol{G}_{\mathrm{I}}^2 \\ \boldsymbol{H}_{\mathrm{I}}^2 \end{bmatrix} \begin{pmatrix} \{\boldsymbol{u}^2\} \\ \{\boldsymbol{u}_{\mathrm{I}}^2\} \end{pmatrix} = \begin{bmatrix} \boldsymbol{B}^2 \\ \boldsymbol{U}_{\mathrm{I}}^2 \\ \boldsymbol{T}_{\mathrm{I}}^2 \end{bmatrix}, \tag{22}$$

for the subdomain Ω_2. In the above equations, the subscript 'I' denotes the interface of the bi-material. $\boldsymbol{U}_{\mathrm{I}}^1$ and $\boldsymbol{T}_{\mathrm{I}}^1$ indicate the displacement and traction boundary conditions of the subdomain Ω_1 on the interface, $\boldsymbol{B}^1$ stand for the known quantities of subdomain Ω_1 on the remaining points of the subdomain, $\boldsymbol{A}^1$, $\boldsymbol{G}_{\mathrm{I}}^1$ and $\boldsymbol{H}_{\mathrm{I}}^1$ are the corresponding LMFS coefficient matrices. Similarly, $\boldsymbol{U}_{\mathrm{I}}^2$ and $\boldsymbol{T}_{\mathrm{I}}^2$ indicate the displacement and traction boundary conditions of the subdomain Ω_2 on the interface, $\boldsymbol{B}^2$ are the known quantities of subdomain Ω_2 on the remaining points. Along the interface of the bi-material, the following displacement continuity and traction equilibrium conditions should satisfy:

$$\boldsymbol{U}_{\mathrm{I}}^1 = \boldsymbol{U}_{\mathrm{I}}^2, \quad \boldsymbol{T}_{\mathrm{I}}^1 = -\boldsymbol{T}_{\mathrm{I}}^2. \tag{23}$$

According to Eqs (21)–(23), the final matrix equation for both of the subdomains can be coupled together as:

$$\begin{bmatrix} \boldsymbol{A}^1 & [\boldsymbol{0}] \\ [\boldsymbol{0}] & \boldsymbol{A}^2 \\ \boldsymbol{G}_{\mathrm{I}}^1 & -\boldsymbol{G}_{\mathrm{I}}^2 \\ \boldsymbol{H}_{\mathrm{I}}^1 & \boldsymbol{H}_{\mathrm{I}}^2 \end{bmatrix} \begin{bmatrix} \begin{Bmatrix} \boldsymbol{u}^1 \\ \boldsymbol{u}_{\mathrm{I}}^1 \end{Bmatrix} \\ \begin{Bmatrix} \boldsymbol{u}^2 \\ \boldsymbol{u}_{\mathrm{I}}^2 \end{Bmatrix} \end{bmatrix} = \begin{bmatrix} \boldsymbol{B}^1 \\ \boldsymbol{B}^2 \\ [\boldsymbol{0}] \\ [\boldsymbol{0}] \end{bmatrix}. \tag{24}$$

By solving the above equations, the displacements at any point inside the domain and along the boundary can be determined. More equations will be added into the equation system in a similar way for other possible subdomains.

4. Numerical results and discussions

Two benchmark numerical examples are examined in this section to verify the accuracy and efficiency of the present multi-domain LMFS method for the stress analysis of elastic bi-materials. In order to evaluate the performance of the present method, the relative error defined below is employed:

$$Relative\ Error=\left[\sum_{k=1}^{M}\left[I_{\text{numer}}(k)-I_{exact}(k)\right]^2\right]^{1/2}\Bigg/\left[\sum_{k=1}^{M}\left[I_{exact}(k)\right]^2\right]^{1/2}, \tag{25}$$

where $I_{\text{numerical}}(k)$ and $I_{exact}(k)$ are the numerical and analytical solutions at the k^{th} calculated point, respectively, M is the number of calculation points tested. In the following two examples, the radius of the fictitious circle for each of the local subdomain is chosen as $R_s = 0.8$. The number of source points associated with the local subdomain is taken to be $M = 15$. The influence of the parameters R_s and M on the overall accuracy of the LMFS method has been discussed in Refs. [49,55]. It was observed that the numerical solutions were relatively insensitive to these two parameters.

4.1. Test problem 1: stress analysis of a finite bi-material plate

The first example considered here is the stress analysis of a finite bi-material plate, where L=1 m is the length of the bi-material, $H_{c1} = 0.5\,m$ the thickness of the substrate, and $H_{c2} = 0.1\,m$ the thickness of the layered coating. The geometry of the problem and the nodes distribution of the LMFS model can be found in Figure 3. Similar to Ref. [54], the following exact solutions

$$u_1(\boldsymbol{x}) = \left(\cos(x_1+x_2)+\cos(x_2)+x_2\right)/E,\quad u_2(\boldsymbol{x}) = \left(\sin(x_1+x_2)+x_2+1\right)/E, \tag{26}$$

for the layered coating and

$$u_1(\boldsymbol{x}) = \left(\cos(x_1+x_2)+x_2+1\right)/E,\quad u_2(\boldsymbol{x}) = \left(\sin(x_1+x_2)+\cos(x_2)+x_2\right)/E, \tag{27}$$

for substrate are employed. A Chebyshev collocation scheme proposed by Bai et al. [58] is applied for calculating the particular solutions for the given elastic problem. The Poisson's ratio and elastic modulus of the bi-material are taken to be $\nu = 0.25$ and $E = 200$ GPa. For the numerical implementation, a total of 3600 points are discretized inside the whole computational domain.

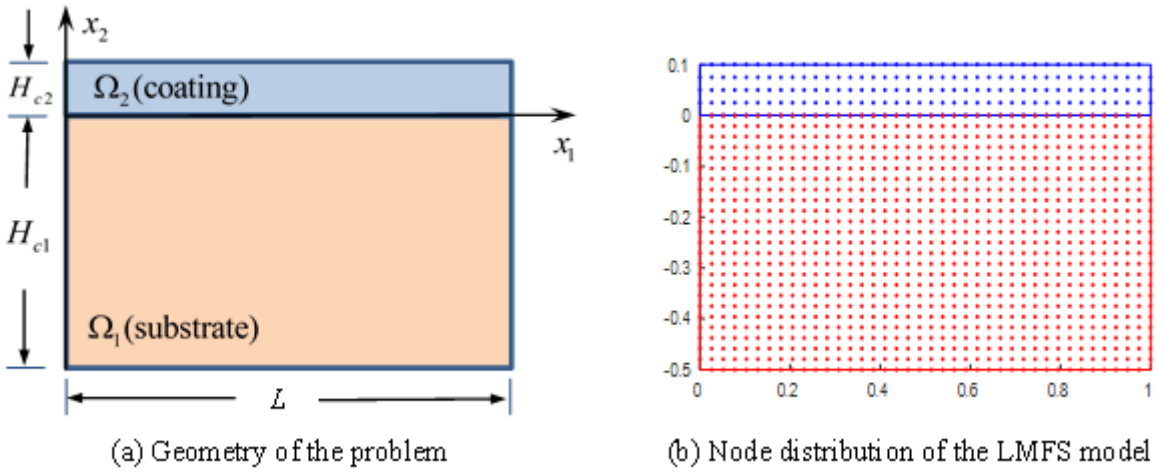

(a) Geometry of the problem (b) Node distribution of the LMFS model

Figure 3. Geometry of the problem (a) and the node distribution of the LMFS model (b).

Figures 4 and 5 show the relative errors of the calculated displacements and stresses at points along the interface of the bi-material. We can observe that the results calculated by using the present LMFS method are in excellent agreement with the corresponding analytical solutions. The LMFS model with only 3600 collocation points are quite accurate for this example, the size of the final system of equations is, therefore, quite small.

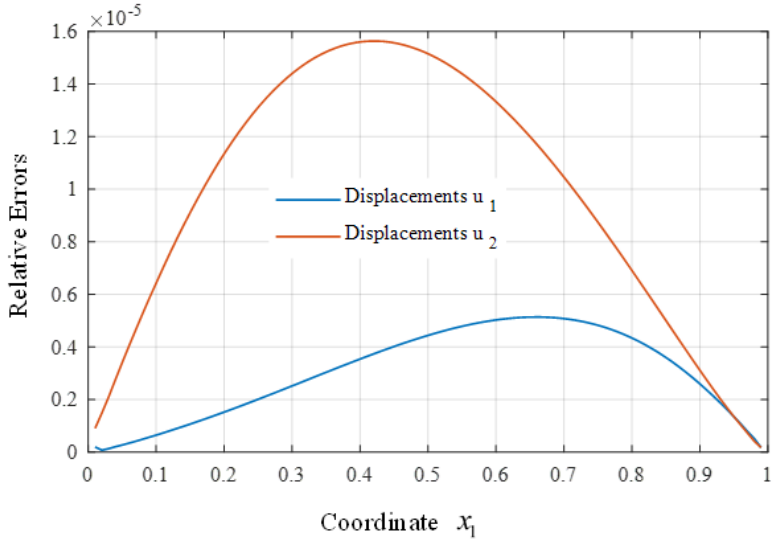

Figure 4. Relative error variation of the calculated displacements at points along the interface of the bi-material.

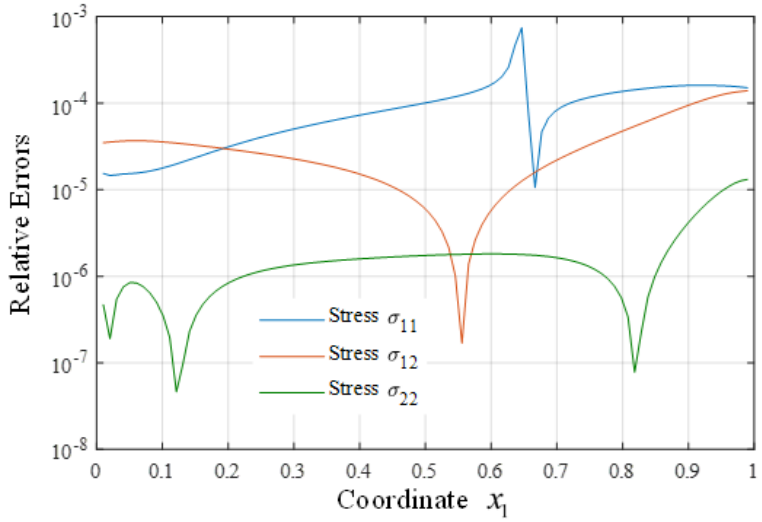

Figure 5. Relative error variation of the calculated stresses at points along the interface of the bi-material.

The distribution of the calculated displacements and the stresses at points inside the whole computational domain are plotted in Figures 6 and 7. These results again are extremely agreement with the corresponding exact solutions. We can conclude that the present LMFS, in conjunction with the

multi-domain technique, can provide stable and accurate numerical solutions for stress analysis of elastic bi-materials.

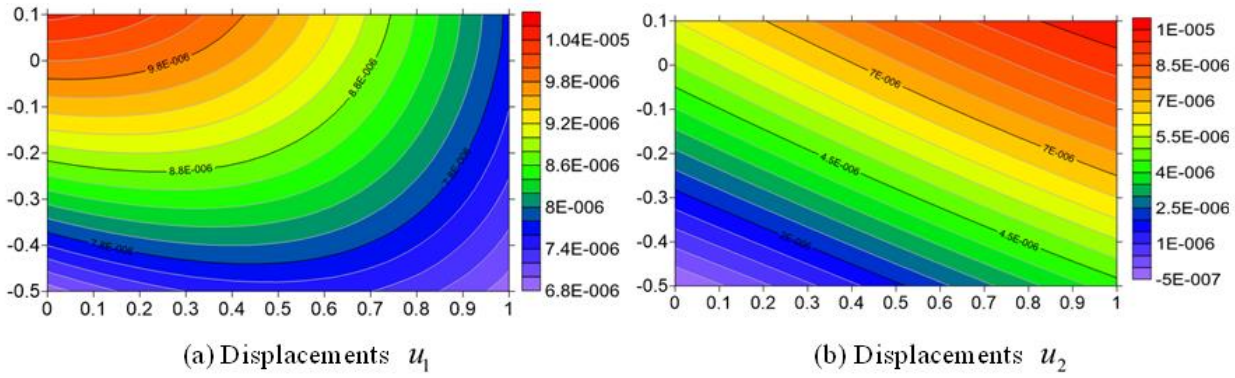

Figure 6. Distribution of the calculated displacements at points inside the whole computational domain.

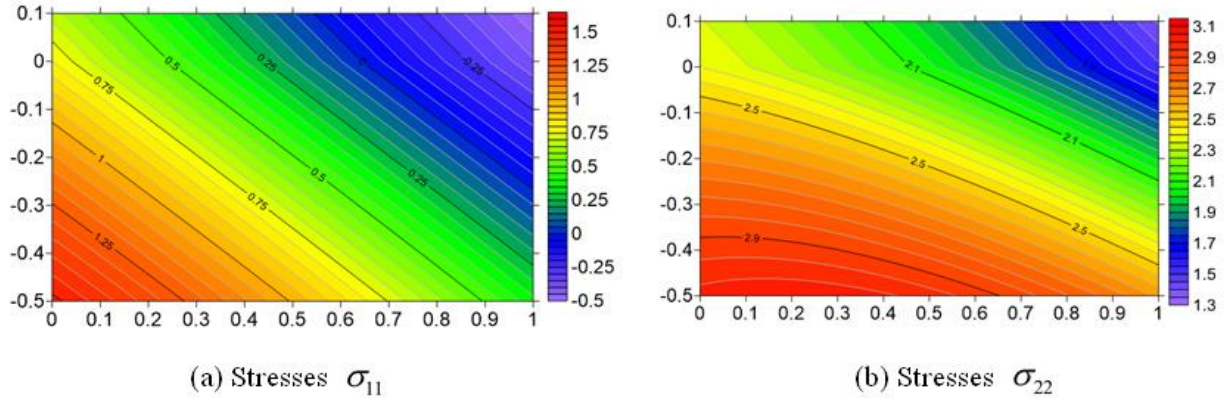

Figure 7. Distribution of the calculated stresses at points inside the computational domain.

4.2. Test problem 2: stress analysis of a circular shaft with two layers of coatings

Here, the stress analysis of a circular shaft with two layers of coatings is considered (see Figure 8). The two coatings consist of two different materials where the Young's modulus of outside coating/Young's modulus of inner coating=1/2 and Poisson ratio of outside coating = Poisson ratio of inner coating $= 0.2$. The substrate and the two layered coatings have radii $r_1 = 5\,m, r_2 = 6\,m$ and $r_3 = 7\,m$, respectively. The system is loaded by a uniform pressure $p = 1\,N$ which is distributed around the surface of the outside coating. The boundary conditions for the displacement, considering the rigid substrate assumption, are $u_r = u_\theta = 0$ at points along the substrate-coating interface, where (r, θ) stands for the polar coordinates. The analytical solutions corresponding to this coating system can be found in Ref. [54,59].

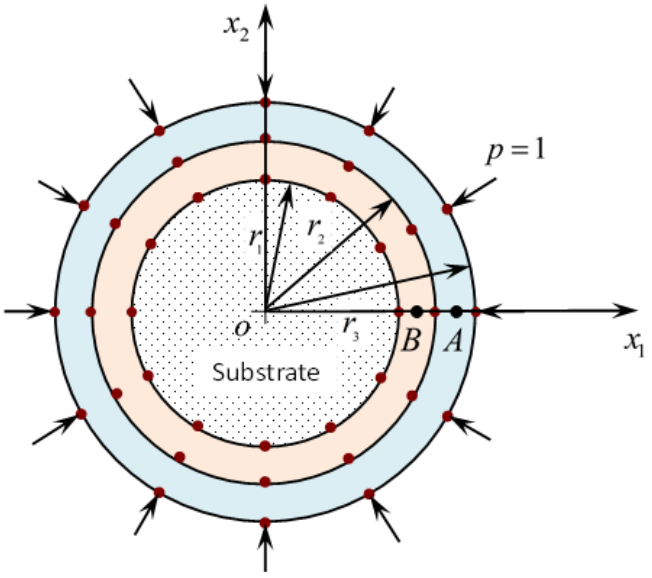

Figure 8. Cross-section of a shaft with two layers of coatings.

To investigate the convergence of the present multi-domain LMFS method, the relative errors of the radial (σ_r) and tangential (σ_θ) stresses at points $A(5.5, 0)$ and $B(6.5, 0)$ are provided in Figure 9, as the number of the LMFS nodes increases from 800 to 15,000. As can be seen from Figure 9, the present LMFS results converge towards their corresponding analytical solutions as the number of nodes increases. In addition, radial and tangential stress results calculated at points along the line $\theta = 0$ are illustrated in Table 1.

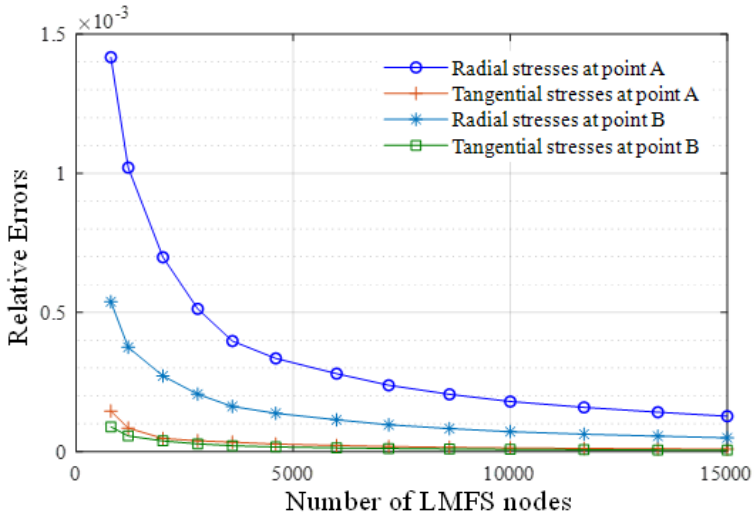

Figure 9. Convergence curves of the calculated radial and tangential stresses at point A and B.

Table 1. Radial and tangential stress results calculated at points along the line $\theta = 0$.

r	Radial stress σ_r			Tangential stress σ_θ		
	Exact solutions	Present	Relative errors	Exact solutions	Present	Relative errors
5.2	−1.2190	−1.2174	1.256E-03	−0.2413	−0.2413	3.568E-04
5.4	−1.1834	−1.1815	1.623E-03	−0.2769	−0.2767	5.621E-04
5.6	−1.1516	−1.1505	9.545E-04	−0.3087	−0.3085	4.256E-04
5.8	−1.1231	−1.1219	1.057E-03	−0.3372	−0.3371	5.521E-04

5. Discussion

This paper makes the first attempt to apply the localized method of fundamental solutions (LMFS) for the stress analysis of two-dimensional (2D) elastic bi-materials. A multi-domain LMFS formulation is proposed to handle the non-homogeneity of the bi-materials. On the subdomain interface, compatibility of displacements and equilibrium of tractions are imposed. Two benchmark examples are well-studied to clarify the accuracy, efficiency and convergency of the present multi-domain LMFS approach. Further analyses are required in order to fully explore the applicability of the new method, including the detailed convergence order analyses of the method as well as the optimal choice of many different parameters. It must be pointed out that the proposed LMFS has many inherent shortcomings compared with the FEM. For example, the method cannot be used for problems whose fundamental solution is either not known or cannot be determined. The method is also not applicable to nonlinear problems for which the principle of superposition does not hold. The method also offers great promise in the analysis of many other problems, including wave propagations, flow problems, non-linear problems. Some work along these lines is already underway.

Acknowledgments

The work described in this paper was supported by the National Natural Science Foundation of China (No. 11802165), the China Postdoctoral Science Foundation (No. 2019M650158), and the Natural Science Foundation of Shandong Province of China (No. ZR2017MF055).

Conflict of interest

The authors declare that they have no known competing financial interests or personal relationships that could have appeared to influence the work reported in this paper.

References

1. A. Karageorghis, D. Lesnic, Steady-state nonlinear heat conduction in composite materials using the method of fundamental solutions, *Comput. Methods Appl. Mech. Eng.*, **197** (2008), 3122–3137. doi: 10.1016/j.cma.2008.02.011.
2. Z. H. Yao, J. D. Xu, H. T. Wang, X. P. Zheng, Simulation of CNT composites using fast multipole BEM, *J. Mar. Sci. Tech.-Taiw.*, **17** (2009), 5. doi: 10.51400/2709-6998.1956.

3. B. T. Johansson, D. Lesnic, A method of fundamental solutions for transient heat conduction in layered materials, *Eng. Anal. Bound. Elem.*, **33** (2009), 1362–1367. doi: 10.1016/j.enganabound.2009.04.014.
4. Y. Gu, W. Chen, C. Zhang, Stress analysis for thin multilayered coating systems using a sinh transformed boundary element method, *Int. J. Solids Struct.*, **50** (2013), 3460–3471. doi: 10.1016/j.ijsolstr.2013.06.018.
5. Y. Gu, C. Zhang, Novel special crack-tip elements for interface crack analysis by an efficient boundary element method, *Eng. Fract. Mech.*, **239** (2020), 107302. doi: 10.1016/j.engfracmech.2020.107302.
6. J. F. Luo, Y. J. Liu, E. J. Berger, Interfacial stress analysis for multi-coating systems using an advanced boundary element method, *Comput. Mech.*, **24** (2000), 448–455. doi: 10.1007/s004660050004.
7. Y.-M. Zhang, Y. Gu, J.-T. Chen, Stress analysis for multilayered coating systems using semi-analytical BEM with geometric non-linearities, *Comput. Mech.*, **47** (2011), 493–504. doi: 10.1007/s00466-010-0559-0.
8. Y. Gu, J. Lei, Fracture mechanics analysis of two-dimensional cracked thin structures (from micro- to nano-scales) by an efficient boundary element analysis, *Results. Appl. Math.*, **11** (2021), 100172. doi: 10.1016/j.rinam.2021.100172.
9. W. Qu, H. He, A spatial–temporal GFDM with an additional condition for transient heat conduction analysis of FGMs, *Appl. Math. Lett.*, **110** (2020), 106579. doi: 10.1016/j.aml.2020.106579.
10. F. Wang, C. Wang, Z. Chen, Local knot method for 2D and 3D convection–diffusion–reaction equations in arbitrary domains, *Appl. Math. Lett.*, **105** (2020), 106308. doi: 10.1016/j.aml.2020.106308.
11. J. Lin, C. S. Chen, C.-S. Liu, J. Lu, Fast simulation of multi-dimensional wave problems by the sparse scheme of the method of fundamental solutions, *Comput. Math. Appl.*, **72** (2016), 555–567. doi: 10.1016/j.camwa.2016.05.016.
12. Z.-J. Fu, J. Zhang, P.-W. Li, J.-H. Zheng, A semi-Lagrangian meshless framework for numerical solutions of two-dimensional sloshing phenomenon, *Eng. Anal. Bound. Elem.*, **112** (2020), 58–67. doi: 10.1016/j.enganabound.2019.12.003.
13. Y. Gu, L. Sun, Electroelastic analysis of two-dimensional ultrathin layered piezoelectric films by an advanced boundary element method, *Int. J. Numer. Meth. Eng.*, **122** (2021), 2653–2671. doi: 10.1002/nme.6635.
14. X. Li, H. Dong, An element-free Galerkin method for the obstacle problem, *Appl. Math. Lett.*, **112** (2021), 106724. doi: 10.1016/j.aml.2020.106724.
15. X. Li, S. Li, A linearized element-free Galerkin method for the complex Ginzburg–Landau equation, *Comput. Math. Appl.*, **90** (2021), 135–147. doi: 10.1016/j.camwa.2021.03.027.
16. G. R. Liu, T. Nguyen-Thoi, H. Nguyen-Xuan, K. Y. Lam, A node-based smoothed finite element method (NS-FEM) for upper bound solutions to solid mechanics problems, *Comput. Struct.*, **87** (2009), 14–26. doi: 10.1016/j.compstruc.2008.09.003.
17. C. S. Chen, H. A. Cho, M. A. Golberg, Some comments on the ill-conditioning of the method of fundamental solutions, *Eng. Anal. Bound. Elem.*, **30** (2006), 405–410. doi: 10.1016/j.enganabound.2006.01.001.

18. H. Xia, Y. Gu, Generalized finite difference method for electroelastic analysis of three-dimensional piezoelectric structures, *Appl. Math. Lett.*, **117** (2021), 107084. doi: 10.1016/j.aml.2021.107084.
19. W. Qu, C.-M. Fan, X. Li, Analysis of an augmented moving least squares approximation and the associated localized method of fundamental solutions, *Comput. Math. Appl.*, **80** (2020), 13–30. doi: 10.1016/j.camwa.2020.02.015.
20. P.-W. Li, Z.-J. Fu, Y. Gu, L. Song, The generalized finite difference method for the inverse Cauchy problem in two-dimensional isotropic linear elasticity, *Int. J. Solids Struct.*, **174–175** (2019), 69–84. doi: 10.1016/j.ijsolstr.2019.06.001.
21. F. J. Wang, C. M. Fan, C. Z. Zhang, J. Lin, A localized space-time method of fundamental solutions for diffusion and convection-diffusion problems, *Adv. Appl. Math. Mech.*, **12** (2020), 940–958. doi: 10.4208/aamm.OA-2019-0269.
22. W. Qu, Y. Gu, Y. Zhang, C.-M. Fan, C. Zhang, A combined scheme of generalized finite difference method and Krylov deferred correction technique for highly accurate solution of transient heat conduction problems, *Int. J. Numer. Meth. Eng.*, **117** (2019), 63–83. doi: 10.1002/nme.5948.
23. W. Qu, W. Chen, Z. Fu, Y. Gu, Fast multipole singular boundary method for Stokes flow problems, *Math. Comput. Simulat.*, **146** (2018), 57–69. doi: 10.1016/j.matcom.2017.10.001.
24. F. Wang, Y. Gu, W. Qu, C. Zhang, Localized boundary knot method and its application to large-scale acoustic problems, *Comput. Methods Appl. Mech. Eng.*, **361** (2020), 112729. doi: 10.1016/j.cma.2019.112729.
25. P.-W. Li, Space–time generalized finite difference nonlinear model for solving unsteady Burgers' equations, *Appl. Math. Lett.*, **114** (2021), 106896. doi: 10.1016/j.aml.2020.106896.
26. W. Qu, H. He, A GFDM with supplementary nodes for thin elastic plate bending analysis under dynamic loading, *Appl. Math. Lett.*, **124** (2022), 107664. doi: 10.1016/j.aml.2021.107664.
27. W. Qu, H. Gao, Y. Gu, Integrating Krylov deferred correction and generalized finite difference methods for dynamic simulations of wave propagation phenomena in long-time intervals, *Adv. Appl. Math. Mech.*, **13** (2021), 1398–1417. doi: 10.4208/aamm.OA-2020-0178.
28. C. S. Chen, C. M. Fan, P. H. Wen, The method of approximate particular solutions for solving certain partial differential equations, *Numer. Methods Partial Differential Equtaions*, **28** (2012), 506–522. doi: 10.1002/num.20631.
29. C. J. S. Alves, On the choice of source points in the method of fundamental solutions, *Eng. Anal. Bound. Elem.*, **33** (2009), 1348–1361. doi: 10.1016/j.enganabound.2009.05.007.
30. G. Fairweather, A. Karageorghis, The method of fundamental solutions for elliptic boundary value problems, *Adv. Comput. Math.*, **9** (1998): 69. doi: 10.1023/a:1018981221740.
31. J. Lin, W. Chen, L. Sun, Simulation of elastic wave propagation in layered materials by the method of fundamental solutions, *Eng. Anal. Bound. Elem.*, **57** (2015), 88–95. doi: 10.1016/j.enganabound.2014.11.007.
32. J. R. Berger, A. Karageorghis, The method of fundamental solutions for layered elastic materials, *Eng. Anal. Bound. Elem.*, **25** (2001), 877–886. doi: 10.1016/S0955-7997(01)00002-9.
33. J. R. Berger, A. Karageorghis, P. A. Martin, Stress intensity factor computation using the method of fundamental solutions: mixed-mode problems, *Int. J. Numer. Methods Eng.*, **69** (2007), 469–483. doi: 10.1002/nme.1774.

34. G. C. de Medeiros, P. W. Partridge, J. O. Brandão, The method of fundamental solutions with dual reciprocity for some problems in elasticity, *Eng. Anal. Bound. Elem.*, **28** (2004), 453–461. doi: 10.1016/s0955-7997(03)00099-7.
35. A. Karageorghis, G. Fairweather, The method of fundamental solutions for axisymmetric elasticity problems, *Comput. Mech.*, **25** (2000), 524–532. doi: 10.1007/s004660050500.
36. A. Karageorghis, D. Lesnic, L. Marin, The method of fundamental solutions for the detection of rigid inclusions and cavities in plane linear elastic bodies, *Comput. Struct.*, **106–107** (2012), 176–188. doi: 10.1016/j.compstruc.2012.05.001.
37. A. Karageorghis, D. Lesnic, The method of fundamental solutions for the inverse conductivity problem, *Inverse. Probl. Sci. Eng.*, **18** (2010), 567–583. doi: 10.1080/17415971003675019.
38. A. Karageorghis, D. Lesnic, L. Marin, The method of fundamental solutions for three-dimensional inverse geometric elasticity problems, *Comput. Struct.*, **166** (2016), 51–59. doi: 10.1016/j.compstruc.2016.01.010.
39. Z.-C. Li, H.-T. Huang, M.-G. Lee, J. Y. Chiang, Error analysis of the method of fundamental solutions for linear elastostatics, *J. Comput. Appl. Math.*, **251** (2013), 133–153. doi: 10.1016/j.cam.2013.03.018.
40. Q. G. Liu, B. Šarler, Non-singular Method of Fundamental Solutions for anisotropic elasticity, *Eng. Anal. Bound. Elem*., **45** (2014), 68–78. doi: 10.1016/j.enganabound.2014.01.020.
41. Q. G. Liu, B. Šarler, A non-singular method of fundamental solutions for two-dimensional steady-state isotropic thermoelasticity problems, *Eng. Anal. Bound. Elem.*, **75** (2017), 89–102. doi: 10.1016/j.enganabound.2016.11.010.
42. Q. G. Liu, B. Šarler, Non-singular method of fundamental solutions for elasticity problems in three-dimensions, *Eng. Anal. Bound. Elem.*, **96** (2018), 23–35. doi: 10.1016/j.enganabound.2018.07.018.
43. B. Sarler, Q. G. Liu, Non-singular method of fundamental solutions for two-dimensional isotropic elasticity problems, *Comput. Model. Eng. Sci.*, **91** (2013), 235–266. doi: 10.3970/cmes.2013.091.235.
44. L. Marin, Regularized method of fundamental solutions for boundary identification in two-dimensional isotropic linear elasticity, *Int. J. Solids Struct.*, **47** (2010), 3326–3340. doi: 10.1016/j.ijsolstr.2010.08.010.
45. L. Marin, D. Lesnic, The method of fundamental solutions for the Cauchy problem in two-dimensional linear elasticity, *Int. J. Solids Struct.*, **41** (2004), 3425–3438. doi: 10.1016/j.ijsolstr.2004.02.009.
46. A. Poullikkas, A. Karageorghis, G. Georgiou, The method of fundamental solutions for three-dimensional elastostatics problems, *Comput. Struct.*, **80** (2002), 365–370. doi: 10.1016/s0045-7949(01)00174-2.
47. C. M. Fan, Y. K. Huang, C. S. Chen, S. R. Kuo, Localized method of fundamental solutions for solving two-dimensional Laplace and biharmonic equations, *Eng. Anal. Bound. Elem.*, **101** (2019), 188–197. doi: 10.1016/j.enganabound.2018.11.008.
48. Y. Gu, C.-M. Fan, W. Qu, F. Wang, C. Zhang, Localized method of fundamental solutions for three-dimensional inhomogeneous elliptic problems: theory and MATLAB code, *Comput. Mech.*, **64** (2019), 1567–1588. doi: 10.1007/s00466-019-01735-x.

49. Y. Gu, C.-M. Fan, W. Qu, F. Wang, Localized method of fundamental solutions for large-scale modelling of three-dimensional anisotropic heat conduction problems – Theory and MATLAB code, *Comput. Struct.*, **220** (2019), 144–155. doi: 10.1016/j.compstruc.2019.04.010.
50. W. Qu, C.-M. Fan, Y. Gu, F. Wang, Analysis of three-dimensional interior acoustic fields by using the localized method of fundamental solutions, *Appl. Math. Model.*, **76** (2019), 122–132. doi: 10.1016/j.apm.2019.06.014.
51. Y. Gu, M. V. Golub, C.-M. Fan, Analysis of in-plane crack problems using the localized method of fundamental solutions, *Eng. Fract. Mech.*, **256** (2021), 107994. doi: 10.1016/j.engfracmech.2021.107994.
52. Y. Gu, C.-M. Fan, Z. Fu, Localized method of fundamental solutions for three-dimensional elasticity problems: Theory, *Adv. Appl. Math. Mech.*, **13** (2021), 1520–1534. doi: 10.4208/aamm.OA-2020-0134.
53. Y. Wang, Y. Gu, J. Liu, A domain-decomposition generalized finite difference method for stress analysis in three-dimensional composite materials, *Appl. Math. Lett.*, **104** (2020), 106226. doi: 10.1016/j.aml.2020.106226.
54. Y. Wang, Y. Gu, C.-M. Fan, W. Chen, C. Zhang, Domain-decomposition generalized finite difference method for stress analysis in multi-layered elastic materials, *Eng. Anal. Bound. Elem.*, **94** (2018), 94–102. doi: 10.1016/j.enganabound.2018.06.006.
55. Y. Gu, C.-M. Fan, R.-P. Xu, Localized method of fundamental solutions for large-scale modeling of two-dimensional elasticity problems, *Appl. Math. Lett.*, **93** (2019), 8–14. doi: 10.1016/j.aml.2019.01.035.
56. Y. Gu, C. Zhang, Fracture analysis of ultra-thin coating/substrate structures with interface cracks, *Int. J. Solids Struct.*, **225** (2021), 111074. doi: 10.1016/j.ijsolstr.2021.111074.
57. S. Liu, P.-W. Li, C.-M. Fan, Y. Gu, Localized method of fundamental solutions for two- and three-dimensional transient convection-diffusion-reaction equations, *Eng. Anal. Bound. Elem.*, **124** (2021), 237–244. doi: 10.1016/j.enganabound.2020.12.023.
58. Z.-Q. Bai, Y. Gu, C.-M. Fan, A direct Chebyshev collocation method for the numerical solutions of three-dimensional Helmholtz-type equations, *Eng. Anal. Bound. Elem.*, **104** (2019), 26–33. doi: 10.1016/j.enganabound.2019.03.023.
59. Y. Gu, W. Chen, X. Q. He, Domain-decomposition singular boundary method for stress analysis in multi-layered elastic materials, *CMC-Comput. Mater. Con.*, **29** (2012), 129–154. doi: 10.3970/cmc.2012.029.129.

AIMS Press